Morphology and conduction properties of graphite-filled immiscible PVDF/PPgMA blends

Author's version
Published in
Polymers for Advanced Technologies 23(12), pp 1572-1579
DOI: 10.1002/pat.3031
http://dx.doi.org/10.1002/pat.3031

Morphology and Conduction Properties of Graphite Filled Immiscible PVDF/PPgMA Blends

Alberto Fina[1,*], Zhidong Han[1,†], Guido Saracco[1], Ulrich Gross[2], Michael Mainil[3]

1- Dipartimento di Scienza dei Materiali e Ingegneria Chimica, Politecnico di Torino. V.le Teresa Michel, 5, 15121, Alessandria, Italy

2- Institut fuer Waermetechnik und Thermodynamik, Technische Universitaet Bergakademie Freiberg. Gustav-Zeuner-Straße 7, 09596, Freiberg, Germany

3- Nanocyl S.A. Rue de l'Essor, 4, 5060, Sambreville, Belgium

Abstract

Graphite was dispersed in immiscible polyvinylidene fluoride/maleated polypropylene (PVDF/PPgMA) blends to improve the electrical and thermal conductive properties by building double percolation structure. The morphology of PVDF/PPgMA blends was first investigated for several compositions by selective solvent extraction, scanning electron microscopy (SEM) and dynamic mechanical thermal analysis (DMTA). Blends of PVDF and PPgMA were prepare in different relative fractions and PVDF/PPgMA

* Corresponding author. Email: alberto.fina@polito.it. Tel: +39 0131 229316. Fax: +39 0131 229399

† Visiting professor from School of Materials Science and Engineering, Harbin University of Science and Technology. Linyuan Road 4, Dongli District, 150040, Harbin, China. Permanent email address: harbinzhidonghan@yahoo.com.cn

ratio of 7/3 showed well co-continuous structure. Based on this blend, the morphology and properties of composites with different concentration of graphite were investigated to prepare double percolated structures. Graphite was observed to selectively localize in PPgMA phase. The electrical and thermal conductive properties of graphite containing blends were measured, showing enhanced conductivity for the double percolation structures compared with single polymer composites containing the same graphite loadings.

Keywords

Thermal conductivity; electrical conductivity; graphite; double percolation; cocontinuous blends.

1. Introduction

Heterogeneous morphologies, such as dispersed morphology and co-continuous morphology, are usually observed when melt blending two immiscible polymers [1,2]. Of all possible morphologies, co-continuous blends involving the co-existence of at least two continuous structures are of great importance since they combine the properties of continuous phase for both components [3]. Several important factors including compositions (such as volume fraction), structural parameters of the constituent polymers (such as interfacial tension and viscoelastic properties), processing conditions (such as frequency, shear rate and mixing time) play a critical role in the development of co-continuous morphology [4,5]. Co-continuous morphology is usually observed in a certain concentration range around phase inversion which is defined as a the condition where both blend phases reach the maximum continuity [3,6,7]. Several semi-empirical models to predict the phase inversion were proposed on the basis of viscosity, elasticity, and torque [3,8]. Recently, attentions have been paid to building co-continuous structure by controlling the percolation network of conductive fillers in conductive polymer composites (CPC) [9,10,11]. Percolation is generally considered as a

critical filler loading where the first three-dimensional continuous conductive network is built throughout the polymer matrix [12,13]. For co-continuous CPC, the selective location of conductive fillers in one phase or at the interface gives the opportunity to decrease the percolation threshold to a very low level [14,15]. Double percolation is adopted to describe the heterogeneous distributed structure of conductive fillers in the co-continuous composites, where both the percolation network in filler-rich phase and the continuity of this phase in the composites are basic requirements for a conductive network through the composites [16,17].

From a practical point of view, a low percolation threshold offers the possibility to obtain conductive composites with excellent mechanical and processing properties. Much effort has been devoted to design and preparation of double percolated structures by controlling the location of conductive fillers preferably in the minor phase or at the interface of immiscible polymer blends [18]. A significant reduction in the percolation concentration has been realized by selective localization of carbon black (CB) in co-continuous composites [19,20,21]. Similarly, the electrical conductivity of co-continuous high density polyethylene/ethylene-vinyl acetate copolymer (HDPE/EVA) composites was greatly improved by graphite nanosheet preferentially distributed in HDPE [22] and the percolation threshold of silver nanoparticles was decreased by one half taking advantage of co-continuous structure in HDPE/polybutylene terephtalate (PBT) composites [23]. The same approach was applied to carbon nanotubes polymer nanocomposites. Bulk electrical conductivity of polypropylene/acrylonitrile-butadiene-styrene (PP/ABS) blends with multiwall carbon nanotubes (MWNT) showed lower percolation threshold in the co-continuous blends [11]. Similar results were reported on PC/ABS blends, showing lower electrical resistivity as compared to PC or SAN composites with the same MWNT content, i.e. reaching electrical percolation at a lower CNT content [24]. Blends prepared by melt mixing polycarbonate (PC) /MWNT masterbatch with polyethylene (PE) showed a drop of several orders of magnitude in electrical resistivity as soon as the cocontinuous structure is obtained [25,26], the CNT being mainly located in the PC phase. Further improved electrical conductivity was reported for blends between PC containing

MWNT and PP containing montmorillonite, explained by a higher confinement of CNT in the PC phase induced by the presence of clay platelets at the blend interface [27].

The double percolation concept can in principle be applied to the enhancement of thermal conductivity in immiscible polymer blends with low loading level of thermally conductive fillers; however, the only attempts at present to obtain co-continuous blends with a thermally conductive phase were reported by Droval et al. using a syndiotactic polystyrene filled with boron nitride or aluminum oxide, in combination with an electrically conductive phase, for electrothermal applications [28,29,30]. Due to the fact that polymers typically exhibit very low thermal conductivity, it is of interest to obtain thermally conductive composites for some applications, including circuit boards, heat exchangers, electronics appliances and machinery [31,32,33,34].

Poly(vinylidene fluoride) (PVDF) is an important engineering plastic and has been widely investigated thanks to its good mechanical properties, high dielectric permittivity and unique pyroelectric and piezoelectric properties [35]. PVDF was reported to form co-continuous composites with many polymers, such as PMMA [14], HDPE [36] and PP [37]. Attentions have been paid to the electrical conductivity of the composites rather than the thermal conductivity. Electrical percolation threshold as low as 0.037 volume fraction of CB was observed in the PVDF/HDPE composites with double percolation structure [36] and 0.02 in PVDF/PP composites [37] ,which was much lower than that for conventional CB-filled polymer composites. In the present work, the preparation of co-continuous blends of PVDF with maleated polypropylene (PPgMA) is addressed. Hence, a series of compositions are adopted to prepare PVDF/PPgMA blends under certain processing conditions, and their influences on blend morphologies are discussed in terms of continuity index and morphological structure. Graphite is used to enhance the electrical and thermal conductivity of PVDF/PPgMA blends, taking advantage of the high electrical and thermal conductivity of graphite [38,39,40,41]. Double percolation structure in co-continuous composites is investigated by using different graphite concentration and PVDF/PPgMA ratio. The electrical and thermal conductivity of the composites are evaluated in terms of electrical resistivity and thermal diffusivity.

2. Experimental

2.1. Materials

Polyvinylidene fluoride (PVDF, Solef® 1010) with MFI of 2 g/10min (230°C, 2.16kg) was purchased from Solvay Solexis (I). Maleic anhydride grafted polypropylene (PPgMA, Polybond® 3200) with 1.0 wt. % MA and a MFI of 115 g/10 min (190°C, 2.16kg) was purchased from Crompton (US). Graphite (Timrex® KS4) with D90 less than 5 μm was kindly supplied by Timcal (CH). Thickness of the platelets was evaluated by SEM in the range of 100nm. All materials were used as received.

2.2. Sample preparation

The morphology of immiscible polymer blends depends on their compositions as well as the nature of polymers and the processing conditions [42,7]. This paper mainly focuses on the influences of compositions. Thus, samples were prepared under the same conditions by using a twin-screw micro-compounder (DSM, Netherlands) with a mixing chamber of 15 cm^3 and two co-rotating conical screws. Sample preparation was carried out at a screw rotation speed of 100 rpm under nitrogen flow to prevent thermal oxidation during compounding. For PVDF/PPgMA blends, mixing were performed at 210°C for 10 min. For the composites with graphite (KS4), PVDF and PPgMA were first fed into the micro-compounder and blended at 210°C for 3 min, then graphite was fed and the mixing was continued for another 5 min. The materials were then compression moulded using a laboratory press at 220°C for 1 min into desired thick sheets and then cooled under pressure to room temperature.

2.3. Solvent extraction

Selective solvent extraction is a classical method to quantify the phase continuity on a 3D scale [43,44]. Indeed, a polymer in a blend can be completely progressively extracted by its solvent only when it is distributed in a continuous phase, whereas droplets of the same polymer embedded in a second insoluble polymer cannot be extracted. The PVDF

phase was selectively extracted by N,N-dimethylformamide (DMF) at 50°C for 4 h. If the sample disintegrates completely, then PPgMA is considered as fully dispersed in the PVDF matrix and PVDF is considered as 100% continuous. In the case where the sample is not disintegrated, the continuity index (*CI*) of PVDF can be estimated by the ratio of the mass of PVDF dissolved over the total mass of PVDF added to the blend.

$$CI_{PVDF} = \frac{m_{d-PVDF}}{m_{i-PVDF}} \times 100$$

Where m_{d-PVDF} is the dissolved mass of PVDF; m_{i-PVDF} is the initial mass of PVDF in the blend.

2.4. Morphological characterization

The morphology of the materials was observed by optical microscopy (OM), using a Nikon Eclipse LV100D instrument in reflection mode or scanning electron microscopy (SEM) using a LEO 1450 VP instrument, equipped with a back scattered electron detector and EDS elemental analysis INCA Energy 7353 probe. The extruded samples were cut at low temperature (-50°C) to obtain a planar section parallel to the extrusion direction or fractured in liquid nitrogen. SEM samples were then gold coated to ensure surface conductivity during observation.

To observe phase morphology, some fractured samples were etched in DMF (1 h, 50°C) to dissolve the PVDF phase selectively. Partial etching (20 min, 50°C) was performed on PVDF/PPgMA (9/1) to partially extract PVDF and keep the integrity of the sample.

2.5. Dynamic mechanical thermal analysis

Dynamic-mechanical thermal analysis (DMTA) was performed on compression molded films (30 mm × 6 mm × 0.5 mm) in tension film clamp using a TA Q800 instrument. The sample was heated from -50 °C to +160 °C at a heating rate of 2 °C/min and an oscillation frequency of 1 Hz. Strain controlled mode was adopted with a strain of 0.05% (within the range of linear viscoelaticity) and a preload force of 1.0 N.

2.6. Thermal diffusivity measurements

Thermal diffusivity was measured by LFA 427 (Laser Flash Apparatus, Netzsch Gerätebau GmbH, Selb/Germany). Samples with 12.6 mm in diameter and 1 mm in thickness were used, and they were flash heated by the Laser from below. Thermal diffusivity is evaluated from the temperature history of the upper front surface as measured by an infra-red sensor.

2.7. Electrical resistivity measurements

Electrical resistance was tested on either the Keithley 2400 ohmmeter (for VR≤40MΩ) or on the Keithley 2700 ohmmeter (for VR>>1MΩ), on disks sizing 12.6 mm in diameter and 1 mm in thickness. Flat surfaces were coated with electrically conductive paint to ensure electrical contact with the probe.

3. Results and discussion

3.1. PVDF/PPgMA blends

3.1.1. Morphology of PVDF/PPgMA blends

PVDF is well known to be immiscible with PP and PPgMA was proposed as a compatibilizer between PVDF and PP [[45]]. However, when blending PVDF and PPgMA obvious phase separation was observed by SEM, showing clear immiscibility of these two polymers. To investigate the degree of co-continuity, PVDF/PPgMA blends with different compositions were immersed in DMF to selectively extract PVDF. The mass of the bulk solid left after extraction as well as the continuity index of PVDF (defined in the experimental section) is shown in Figure 1 as a function of PPgMA content. After PVDF extraction, PPgMA dispersed in droplets in the PVDF matrix makes no contribution to the mass of bulk solid left, but only continuous PPgMA does. The left mass after extraction from PVDF(90)/PPgMA(10) is close to zero, i.e. PPgMA is removed from the bulk solid residue in the form of fine particles suspended in the solvent. The mass of the bulk residue increases gradually to 37% as the concentration of PPgMA increases to 40 wt.%, suggesting nearly all PPgMA remains in the solid bulk

residue. At 50 wt.% PPgMA, the left mass after extraction amounts to 76%, which is more than the PPgMA content in the blend, indicating the presence of embedded droplets of PVDF in PPgMA matrix, which cannot be extracted. Conversely, the continuity index of PVDF is 100%, i.e. PVDF in the blend is completely extracted, until the concentration of PPgMA is 40 wt.%, then it sharply decreases to about 48% at 50 wt.% PPgMA. Given that a cocontinuous blend is defined as a blend in which both phases are continuous, the results in Figure 1 suggest co-continuous structure in the composition range between 30-40 wt.% PPgMA and the evolution to dispersed domains of PVDF in PPgMA continuous matrix above 40 wt.% PPgMA.

Phase morphology was also studied by SEM on resides obtained after PVDF extraction (Figure 2). As the concentration of PPgMA increases from 10 wt.% to 50 wt.%, the structure of PPgMA phase undergoes a transformation from droplets or fibrils into continuous network. At 10 wt.% PPgMA, dispersed droplets and short fibrils are observable after partial extraction of PVDF (Figure 2a). The blend containing 20 wt.% PPgMA exhibit the big holes left after extraction of PVDF and a continuous structure of PPgMA (Figure 2b), together with some elongated fibrils randomly deposited on the PPgMA skeleton. This suggests the presence of some isolated PPgMA particles in the PVDF matrix, which are freed during PVDF extraction, and confirms the limited PPgMA continuity. Well continuous tridimensional structure of both PPgMA skeleton and holes left by PVDF extraction is observed at 30 and 40 wt.% PPgMA content (Figure 2c and Figure 2d). Further increase of PPgMA concentration leads to dispersed droplets of PVDF in the PPgMA continuous matrix (Figure 2e). As a result, SEM demonstrates the change from cocontinuous to dispersed morphology around 40 wt.% PPgMA, in consistence with the continuity index.

3.1.2. Dynamic mechanical properties of PVDF/PPgMA blends

Dynamic mechanical properties are widely used to investigate phase evolution in immiscible blends thanks to their sensitivity to the phase change [43]. Figure 3 shows the

temperature dependence of storage modulus and tanδ of PVDF/PPgMA blends with different compositions. The storage modulus of the PVDF/PPgMA blend is lower than single PVDF and PPgMA, which might be due to a changed crystallization behaviors of the individual phases in the blends [46], as well as to defects introduced at the PVDF/PPgMA interface. The storage modulus of the blends is always lower than for PVDF in the whole temperature range explored and decreases with the increase of PPgMA concentration in the blend. In particular, a significant modulus drop is found when the concentration of PPgMA increases from 30 to 40 wt.%. Two transitions are observed in the tanδ vs. temperature curves of PPgMA and PVDF: (i) α transition derived from the motions within the crystalline region and (ii) β transition attributed to the glass transition of the amorphous phase [47,48]. Two distinct peaks of tanδ (in Figure 3) each exactly corresponding to the glass transition temperatures of PVDF and PPgMA can be observed in all the blends indicating the immiscibility between the two phases. The glass transition of PVDF (-40°C) and PPgMA (7°C) can be observed in the blends and its intensity is proportional to the relative fractions in the blend. Considering the dependence of the storage modulus on the blend composition, the storage modulus at different temperature as functions of the concentration of PPgMA is shown in Figure 4, aiming to correlate the dynamic mechanical properties with the morphological structure of blends. The storage modulus of the blend can be used to study the phase inversion region in cocontinuous blends, as it typically undergoes a remarkable change in its value across the phase inversion [49]. Considering the glass transition temperatures (T_g) for PVDF (-40°C) and PPgMA (7°C), the temperature dependence of storage modulus at -50°C (below $T_{g,PVDF}$), -10°C (between $T_{g,PVDF}$ and $T_{g,PPgMA}$) and 25°C (room temperature, above $T_{g,PPgMA}$) vs. the concentration of PPgMA were selected and are compared in Figure 4. Storage modulus at different temperature all drastically change between 30 wt.% and 40 wt.% PPgMA, revealing the occurrence of co-continuous structures, as previously reported in literature [49].

3.2. PVDF/PPgMA/graphite composites

3.2.1. Morphology of PVDF/PPgMA/graphite composites

To achieve desired final properties, the control of morphology is crucial. As evidenced above, co-continuous structure can be obtained when the concentration of PPgMA is between 30 and 40 wt.%. To build a network for electrical or thermal transfer at low filler loading, PVDF/PPgMA 7/3 was selected for further research. As a first approach, the ratio between PVDF and PPgMA was kept constant and graphite was added at different concentration (10, 20, 30 wt.%). The micrographs obtained by optical microscopy on cryo-cut surfaces are shown in Figure 5.

In all blends, a clear phase separation is observable and graphite, observable as shiny particle when observed in reflected light, appears to be selectively located in the minoritary phase (i.e. PPgMA). The selective distribution of fillers in immiscible blends depends both on thermodynamics and kinetics of mixing [50]. In PVDF/PP blends, CB was previously found to locate in the PP phase rather than the PVDF phase [37], revealing the stronger affinity of CB particles to the PP phase. The similarity in composition between graphite and carbon black may suggest an obvious interpretation of graphite selective location based on elemental interaction parameters. However, kinetic effects are also expected to play a role: in particular, the significantly lower viscosity of PPgMA compared to PVDF is likely to result in an easier adsorption of PPgMA on graphite platelets rather than of PVDF.

At 10wt.% graphite loading (Figure 5a), the microstructure of graphite containing phase is very coarse, with coexistence of very large domains (hundreds of μm) with limited continuity and isolated droplets (tens of μm). When increasing graphite to 20wt.%, a completely different microstructure is observed (Figure 5b), with finer phase separation and high degree of continuity for both phases to determine an effective co-continuous network. With further increase of graphite loading to 30wt.%, a much finer structure (few μm) is obtained and the phase separation is not clearly observable (Figure 5c). Similar blend structure refinement with increasing of inorganic filler concentration has been previously reported for different nanoparticles in blends [21,51,52]. In the present case, due to the micronic size of graphite platelets, excessive refinement

of the blend structure is to be avoided, as particles can cause defects of continuity when phase separation becomes comparable to the size of graphite platelets. From these results, the ratio between PPgMA and graphite appears to control phase morphology. To further investigate this issue, a composite having a graphite loading of 10 wt.% and reduced relative amount of PPgMA (13.5%) was also prepared for comparison and microstructure is reported in Figure 5d. It is clearly observable that graphite containing domains present very elongated shape and some degree of continuity into the continuous matrix. Such a bidimensional structure is expected to correspond to a certain degree of co-continuity in the three dimension, which cannot be fully appreciated from 2D micrographs. These results confirm that the loading of fillers into the host polymer controls the microstructure, likely owing to the change in viscosity, in agreement with the classical theory for co-continuous blends [3].

SEM analysis was performed on fragile-fracture surfaces to gain some more insight about the 3D structure of co-continuous blends. Figure 6 show the microstructure of PVDF(56)/PPgMA(24)/Graph(20): graphite platelets are clearly observable in PPgMA phase only, as confirmed by EDS analysis and continuity of both phases can be appreciated thanks to the high depth of field of SEM images. Debonding at the interfaces can also be observed, owing to limited compatibility between the two polymers.

3.2.2. Electrical and Thermal conductivity of PVDF/PPgMA/graphite composites

The electrical conductivity of PVDF/PPgMA/graphite composites was calculated from measured resistance. The results are collected in Table 2 and reported in Figure 7. Compared with PVDF or PPgMA (conductivity in the range of 10^{-14} S/cm), the conductivity of the composites dramatically increases (10^{-7}~10^{-2} S/cm), revealing the obvious improvement of electrical conductivity of the composites.

Within co-continuous blends containing graphite, electrical conductivity is strongly increased by the increase in graphite content. In particular, an increase by four orders of

magnitude was obtained increasing graphite content from 10% to 20%, which is attributed to a higher co-continuity degree, in addition to the obvious effect of the higher conductive particle content. Interestingly, with 30% graphite in the blend, the value of electrical conductivity is comparable with the simple composite PPgMA(55)/Graph(45), despite the lower graphite content. This is explainable with the higher local concentration of graphite in PPgMA phase, which determines a high number of contacts between particles effective in electron transport. Similar results were also reported for electrical conductivity in a PVDF/HDPE blend filled with carbon black by Feng and Chan [[36]]. As a result of Figure 7, the percolation threshold of about 20 wt.% graphite was observed in the co-continuous blend composites, lower than about 30 wt.% graphite in single polymer composites. Thanks to the confinement of graphite in PPgMA phase (Figure 6), the local concentration of graphite in PVDF(56)/PPgMA(24)/Graph(20) can be calculated as 45.5 wt.%, which closely compares to the blend PPgMA(55)/Graph(45). Electrical conductivity for these two composites are $3.9*10^{-3}$ and $2.1*10^{-2}$ S/cm, respectively. However, in the single-polymer composites, the full volume of the sample is conductive, whereas only a fraction of the volume contributes to electron transfer in the polymer blend. Excluding the volume of insulating polymer (PVDF, about 46 vol.%) and taking into account that the structure of PPgMA/graphite is not perfectly continuous (some isolated domains in PVDF are possible) the two difference between the two measured conductivity values further decreases. These findings suggest the efficiency of thermal contact in the conductive phase of PVDF(56)/PPgMA(24)/Graph(20) to be very similar to the one in PPgMA(55)/Graph(45).

When comparing blends PVDF(63)/PPgMA(27)/Graph(10) with PVDF(77)/PPgMA(13)/Graph(10), one can further observe the effect of the local concentration of graphite while keeping the same overall concentration of conductive particles. Indeed, when increasing the local concentration of graphite from 27% to 43.5%, an increase of electrical conductivity by about two orders of magnitude was obtained. This may be explained by the higher number of contacts between conductive particles, which are selectively segregated in the PPgMA phase. However, the

conductivity performance depends also on the degree of co-continuity in the blend, which can also contribute to the difference in conductivity for the two blends, as previously reported for PVDF/PP/CB composites [37].

Comparison between co-continuous blend composite PVDF(49)/PPgMA(21)/Graph(30) with simple composite PVDF(70)/Graph(30) containing the same overall graphite content shows better conductivities for the cocontinuous blend, further confirming the advantage obtained when segregating conductive particles in a confined volume.

Thermal conductivity of composites was also evaluated in terms of thermal diffusivity, reported in Table 2. As the graphite concentration increases from 10% to 30% in the composites with PVDF/PPgMA ratio of 7/3, thermal diffusivity increases nearly linearly, to a value of 0.362 mm^2s^{-1} with 30% graphite. Unlike electrical resistivity, thermal diffusivity of the composites does not go through a sharp change even though these composites have been proved of co-continuous structure, in agreement with previously reported results [28,53]. This is explained by the fact that the ratio between filler and matrix conductivities is typically in the range of 10^{16} for electrical transport and in the range of 10^3 for thermal transport. Furthermore, the efficiency of contact between particles is related to the mechanisms of conduction. Electrical conductivity is based on electron transmission, which is possible by tunnel effect when two particles are close enough, whereas a phonon (responsible for thermal transfer) requires strong vibrational coupling between the particles for effective heat transmission through the contact. The problem of thermal contact between particles resulting in very low efficiency of particle-particle heat transfer, is discussed extensively elsewhere [31].

Comparing thermal diffusivity for PVDF(70)/Graph(30) with PVDF(49)/PPgMA(21)/Graph(30) and PVDF(56)/PPgMA(24)/Graph(20), it clearly turns out that segregation of the conductive particles in the minor phase is beneficial for thermal conductivity. Indeed, a significantly higher diffusivity is obtained for the blend composite compared the simple PVDF-based composite with the same graphite loading, while similar performance is obtained with lower (20%) loading. Differences in the

increase in thermal diffusivity vs. graphite content between single polymer composites and cocontinuous blend composites are clearly shown in Figure 8.

Similarly to electrical conductivity, this is attributed to the higher number of contacts between conductive particles. Moreover, for thermal transfer, the segregation of conductive particles in a restricted volume might also play a role in the efficiency of thermal contact [31]. Comparing PVDF(63)/PPgMA(27)/Graph(10) with PVDF(77)/PPgMA(13)/Graph(10)similar thermal diffusivity results are observed in spite of it higher local graphite concentration, which does not follow the same trend obtained for electrical conductivity of two composites. As observed in Figure 5d, PVDF(77)/PPgMA(13)/Graph(10) showed very elongated domains and only some degree of co-continuity. This morphology might account for the different trends in its electrical and thermal conductivity. Since the transfer of phonons depends much on the interface structure and thermal contact of the particle, the degree of co-continuity will exert more significant influence on thermal conductivity than electrical conductivity.

Conclusions

The morphology of PVDF/PPgMA blends prepared by melt mixing was studied for PPgMA content ranging from 10wt.% to 50wt.% by selective solvent extraction coupled with SEM and DMTA, showing the formation of well co-continuous structure in blend containing 30 wt.% PPgMA.

When adding graphite particles to the blends, these selectively locate in the PPgMA phase. On the other hand, the co-continuity of the blend having PVDF/PPgMA ratio 7/3 is retained in the presence of graphite up to graphite loading of 30%, evidencing the formation of a double percolated structure. Furthermore, a progressive refinement of the phase separation was observed with increasing graphite content, down to a few micron range for 30wt.% graphite loading.

Electrical and thermal conductivities for the blends were evaluated, clearly showing better performance of the double percolation structures compared with single polymer composites containing the same graphite loadings, for both electrical and

thermal conductivities.

Acknowledgements

The authors are grateful to Prof. Giovanni Camino at Politecnico di Torino for discussion and support during the preparation of this work. A special thanks goes to Mr. Samuele Colonna for compounding and specimens preparations. A. Fina also thanks Dr. Donald R. Paul at the University of Texas at Austin for the useful discussions on polymer blends preparation.

The research leading to this results has received funding from the European Community's Seventh Framework Programme (FP7 2007-2013) under grant agreement n° 227407 – Thermonano.

Z. Han is grateful to the Post-Doc Fellowship for Senior Researcher programme of Politecnico di Torino for financial support.

References

[1] Lee JK, Han CD. Evolution of a dispersed morphology from a co-continuous morphology immiscible polymer blends. Polymer 1999;40(10):2521-2536.

[2] Lyngaae-Jørgensen J, Utracki LA. Structuring polymer blends with bicontinuous phase morphology. Part II. Tailoring blends with ultralow critical volume fraction. Polymer 2003;44(5):1661-1669.

[3] Pötschke P, Paul DR. Formation of Co-continuous structures in melt-mixed immiscible polymer blends. J Macromol Sci C: Polym Rev 2003;43(1):87-141.

[4] Chuai CZ, Almdal K, Johannsen I, Lyngaae-Jørgensen J. Morphology evolution of polycarbonate-polystyrene blends during compounding. Polymer 2001;42(19):8217-8223.

[5] Veenstra H, Van Dam J, Posthuma de Boer A. Formation and stability of co-continuous blends with a poly(ether-ester) block copolymer around its order-disorder temperature. Polymer 2000;41(8):3037–3045.

[6] Lazo NDB, Scott CE. Morphology development during phase inversion of a PS PE blend in isothermal, steady shear flow. Polymer 1999;40(20):5469–5478.

[7] Mekhilef N, Verhoogt H. Phase inversion and dual-phase continuity in polymer blends: Theoretical predictions and experimental results. Polymer 1996;37(18):4069-4077.

[8] Steinmann S, Gronski W, Friedrich C. Cocontinuous polymer blends: influence of viscosity and elasticity ratios of the constituent polymers on phase inversion. Polymer 2001;42(15):6619-6629.

[9] Bose S, Bhattacharyya AR, Kulkarni AR, Pötschke P. Electrical, rheological and morphological studies in co-continuous blends of polyamide 6 and acrylonitrile-butadiene-styrene with multiwall carbon nanotubes prepared by melt blending. Comp Sci Tech 2009;69(3-4):365-372.

[10] Xu S, Wen M, Li J, Guo S, Wang M, Du Q, Shen J, Zhang Y, Jiang S. Structure and properties of electrically conducting composites consisting of alternating layers of pure polypropylene and polypropylene with a carbon black filler. Polymer 2008;49(22):4861-4870.

[11] Khare RA, Bhattacharyya AR, Kulkarni AR, Saroop M, Biswas A. Influence of

Multiwall Carbon Nanotubes on Morphology and Electrical Conductivity of PP/ABS Blends. J Polym Sci Part B: Polym Phys 2008;46(21):2286-2295.

[12] Yui H, Wu G, Sano H, Sumita M, Kino K. Morphology and electrical conductivity of injection-molded polypropylene/carbon black composites with addition of high-density polyethylene. Polymer 2006;47(10):3599-3608.

[13] Zhang C, Wang P, Ma C, Wu G, Sumita M. Temperature and time dependence of conductive network formation: Dynamic percolation and percolation time. Polymer 2006;47(1):466-473.

[14] Wu G, Miura T, Asai S, Sumita M. Carbon black-loading induced phase fluctuations in PVDF/PMMA miscible blends: dynamic percolation measurements. Polymer 2001;42(7):3271-3279.

[15] Al-Saleh MH, Sundararaj U. An innovative method to reduce percolation threshold of carbon black filled immiscible polymer blends. Compos Part A-Appl S 2008;39(2):284-293.

[16] Cheah K, Forsyth M, Simon GP. Conducting composite using an immiscible polymer blend matrix. Synthetic Met 1999;102(1-3):1232-1233.

[17] Thongruang W, Spontak RJ, Balik CM. Bridged double percolation in conductive polymer composites: an electrical conductivity, morphology and mechanical property study. Polymer 2002;43(13):3717-3725.

[18] Mironi-Harpazi, Arkis M. Electrical behavior and structure of polypropylene/ultrahigh molecular weight polyethylene/carbon black immiscible blends. Journal of Applied Polymer Science, 2001, 81: 104–115.

[19] Al-Saleh MH, Sundararaj U. Nanostructured carbon black filled polypropylene/polystyrene blends containing styrene-butadiene-styrene copolymer: Influence of morphology on electrical resistivity. Eur Polym J 2008;44(7):1931-1939.

[20] Zhang QH, Chen DJ. Percolation threshold and morphology of composites of conducting carbon black/polypropylene/EVA. J Mater Sci 2004;39(5):1751-1757.

[21] Hom S, Bhattacharyya AR, Khare RA, Kulkarni AR, Saroop M, Biswas A. PP/ABS Blends with Carbon Black: Morphology and Electrical Properties. J Appl Polym Sci 2009;112(2):998-1004.

[22] Chen G, Lu J, Wu D. The electrical properties of graphite nanosheet filled immiscible polymer blends. Mater Chem Phys 2007;104(2-3):240-243.

[23] Rybak A, Boiteux G, Melis F, Seytre G. Conductive polymer composites based on

metallic nanofiller as smart materials for current limiting devices. Compos Sci Tech 2010;70(2):410-416.

[24] Andreas Göldel, Gaurav Kasaliwal, and Petra Pötschke, "Selective Localization and Migration of Multiwalled Carbon Nanotubes in Blends of Polycarbonate and Poly(styrene-acrylonitrile).," *Macromolecular rapid communications* 30, no. 6 (March 19, 2009): 423-9, http://doi.wiley.com/10.1002/marc.200800549.

[25] Pötschke P, Bhattacharyya AR, Janke A. Morphology and electrical resistivity of melt mixed blends of polyethylene and carbon nanotube filled polycarbonate. Polymer 2003;44(26):8061-8069.

[26] Pötschke P, Bhattacharyya AR, Janke A. Carbon nanotube-filled polycarbonate composites produced by melt mixing and their use in blends with polyethylene. Carbon 2004;42(5-6):965-969.

[27] Pötschke P, Kretzschmar B, Janke A. Use of carbon nanotube filled polycarbonate in blends with montmorillonite filled polypropylene. Compos Sci Tech 2007;67(5):855-860.

[28] Droval G, Feller JF, Salagnac P, Glouannec P. Thermal conductivity enhancement of electrically insulating syndiotactic poly(styrene) matrix for diphasic conductive polymer composites. Polym Adv Technol 2006;17(9-10):732-745.

[29] Droval G, Feller JF, Salagnac P, Glouannec P. Conductive polymer composites with double percolated architecture of carbon nanoparticles and ceramic microparticles for high heat dissipation and sharp PTC switching. Smart Mater Struct 2008;17(2) 025011.

[30] Droval G, Feller JF, Salagnac P, Glouannec P. : Rheological properties of conductive polymer composite (CPC) filled with double percolated network of carbon nanoparticles and boron nitride powder. e-Polymers 2009, no. 023.

[31] Han Z, Fina A. Thermal conductivity of carbon nanotubes and their polymer nanocomposites: A review. Progr Polym Sci, 2011, 36(7): 914-944.

[32] King JA, Tucker KW, Vogt BD, Weber EH, Quan C. Electrically and thermally conductive nylon 6,6. Polym Compos 1999;20(5):643-654.

[33] Raman C, Meneghetti P. Boron nitride finds new applications in thermoplastic compounds. Plastics, Additives and Compounding 2008;10(3):26-31.

[34] Ishida H, Rimdusit S. Very high thermal conductivity obtained by boron nitride-filled polybenzoxazine. Thermochim Acta 1998;320(1-2):177-186.

[35] He F, Fan J, Lau S. Thermal, mechanical, and dielectric properties of graphite reinforced poly(vinylidene fluoride) composites. Polymer Testing, 2008, 27: 964–970.

[36] Feng J, Chan C-M. Carbon Black-Filled Immiscible Blends of Poly(Vinylidene Fluoride) and High Density Polyethylene: Electrical Properties and Morphology. Polymer Engineering and Science. 1998, 38: 1649-1657.

[37] Xu H-P, Dang Z-M, Yao S-H, Jiang M-J, Wang D. Exploration of unusual electrical properties in carbon black/binary-polymer nanocomposites. Applied Physics Letters, 2007, 90: 152912: 1-3.

[38] Pierson HO. Handbook of Carbon, Graphite, Diamond and Fullerences: Properties, Processing and Applications. New Jersey: Noyes Publications, 1993.

[39] Wypych G. Handbook of Fillers: Physical Properties of Fillers and Filled Materials. Toronto: ChemTec Publishing, 2000.

[40] Causin V, Marega C, Marigo A, Ferrara G, Ferraro A. Morphological and structural characterization of polypropylene/conductive graphite nanocomposites. Eur Polym J 2006;42(12):3153-3161.

[41] Tu H, Ye L. Thermal conductive PS/graphite composites. Polym Adv Technol 2009;20(1):21-27.

[42] Willemse RC, de Boer AP, Van Dam J, Gotsis AD. Co-continuous morphologies in polymer blends: the influence of the interfacial tension. Polymer 1999;40(4):827-834.

[43] Omonov TS, Harrats C, Moldenaers P, Groeninckx G. Phase continuity detection and phase inversion phenomena in immiscible polypropylene/polystyrene blends with different viscosity ratios. Polymer 2007;48(20):5917-5927.

[44] Bhadane PA, Champagne MF, Huneault MA, Tofan F, Favis BD. Continuity development in polymer blends of very low interfacial tension. Polymer 2006;47(8):2760–2771.

[45] Dang Z-M, Yan W-T, Xu H-P. Novel high-dielectric-permittivity poly(vinylidenefluoride)/polypropylene blend composites: the influence of the poly(vinylidene fluoride) concentration and compatibilizer. Journal of Applied Polymer Science, 2007, 105: 3649-3655.

[46] Varga J, Menyhárd A. Crystallization, melting and structure of polypropylene/poly(vinylidene-fluoride) blends. Journal of Thermal Analysis and Calorimetry, 2003, 73: 735-743.

[47] Järvelä P, Shucai L, Järvelä P. Dynamic mechanical properties and morphology of polypropylene/maleated polypropylene blends. J Appl Polym Sci 1996;62(5):813-826.

[48] Mano JF, Sencadas V, Mello Costa A, Lanceros-Méndez S. Dynamic mechanical analysis and creep behaviour of beta-PVDF films. Mater Sci Eng A 2004;370(1-2):336-340.

[49] Dedecker K, Groeninckx G. Reactive compatibilisation of A/(B/C) polymer blends - Part 2. Analysis of the phase inversion region and the co-continuous phase morphology. Polymer 1998;39(21):4993-5000.

[50] Fenouillot F, Cassagnau P, Majesté J-C. Uneven distribution of nanoparticles in immiscible fluids: Morphology development in polymer blends. Polymer, 2009, 50: 1333–1350.

[51] Li W, Jozsef KK, Thomann R. Compatibilization Effect of TiO2 Nanoparticles on the Phase Structure of PET/PP/TiO2 Nanocomposites. J Polym Sci Part B: Polym Phys 2009;47(16):1616-1624.

[52] Wang K, Wang C, Li J, Su J, Zhang Q, Du R, Fu Q. Effects of clay on phase morphology and mechanical properties in polyamide 6/EPDM-g-MA/organoclay ternary nanocomposites. Polymer 2007;48(7):2144-2154.

[53] Ye M, Boudenne A, Lebovka N, Ibos L, Candau Y, Lisunova M. Electrical and thermophysical behaviour of PVC-MWCNT nanocomposites. Compos Sci Technol 2008;68(9):1981-1988.

Table 1: Composition of formulations prepared

Formulation PVDF/PPgMA/graphite	PVDF/PPgMA ratio	PVDF [%]	PPgMA [%]	Graphite [%]
PVDF(90)/PPgMA(10)	9/1	90	10	-
PVDF(80)/PPgMA(20)	8/2	80	20	-
PVDF(70)/PPgMA(30)	7/3	70	30	-
PVDF(60)/PPgMA(40)	6/4	60	40	-
PVDF(50)/PPgMA(50)	5/5	50	50	-
PVDF(70)/Graph(30)	-	70	-	30
PPgMA(73)/Graph(27)	-	-	73	27
PPgMA(55)/Graph(45)	-	0	55	45
PVDF(63)/PPgMA(27)/Graph(10)	7/3	63	27	10
PVDF(56)/PPgMA(24)/Graph(20)	7/3	56	24	20
PVDF(49)/PPgMA(21)/Graph(30)	7/3	49	21	30
PVDF(77)/PPgMA(13)/Graph(10)	17/3	76.5	13.5	10

Table 2: Electrical and thermal transport properties of PVDF/PPgMA/Graphite composites

Formulation	**Graphite content [wt.%]**	**Content of graphite in host phase [wt.%]**	**Electrical conductivity [S/cm]**	**Thermal diffusivity [mm^2s^{-1}]**
PVDF(100)	-	-	$\approx 10^{-14}$	0.082
PPgMA(100)	-	-	$\approx 10^{-14}$	0.118
PVDF(70)/PPgMA(30)	-	-	$\approx 10^{-14}$	0.105
PPgMA(73)/Graph(27)	27	27	$1.2*10^{-6}$	0.280
PPgMA(55)/Graph(45)	45	45	$2.1*10^{-2}$	0.497
PVDF(70)/Graph(30)	30	30	$3.5*10^{-3}$	0.223
PVDF(63)/PPgMA(27)/Graph(10)	10	27	$2.4*10^{-7}$	0.167
PVDF(56)/PPgMA(24)/Graph(20)	20	45.5	$3.9*10^{-3}$	0.252
PVDF(49)/PPgMA(21)/Graph(30)	30	58.8	$3.4*10^{-2}$	0.362
PVDF(77)/PPgMA(13)/Graph(10)	10	43.5	$6.9*10^{-5}$	0.140

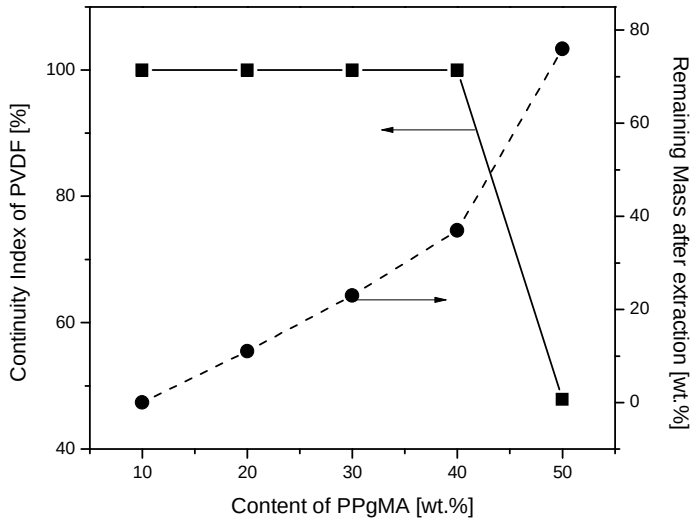

Figure 1: Continuity index of PVDF and left mass after extraction as a function of PPgMA content in the blends

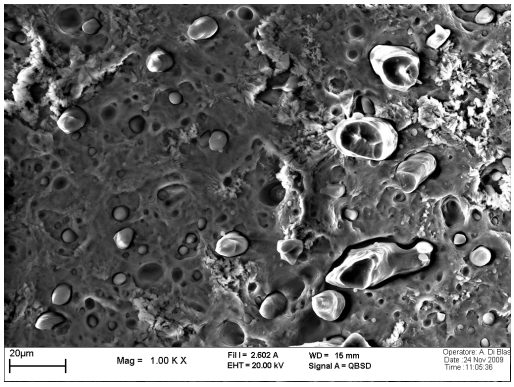

(a)

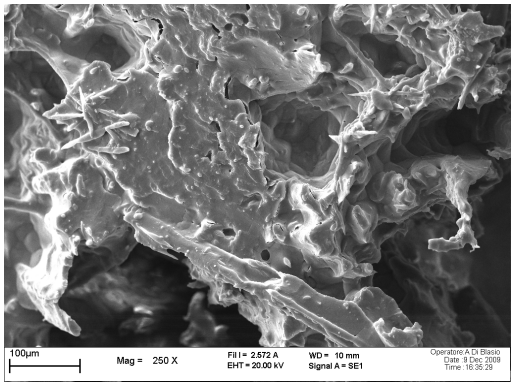

(b)

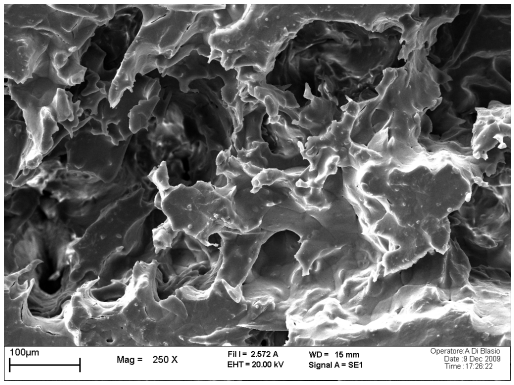

(c)

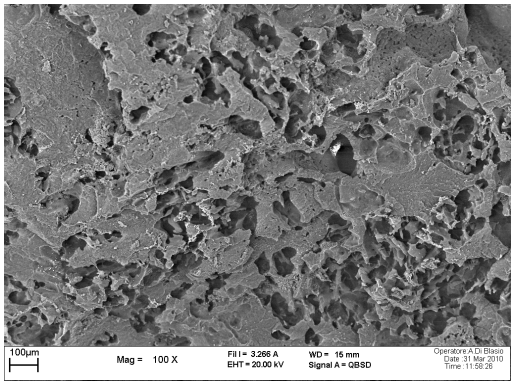

(d)

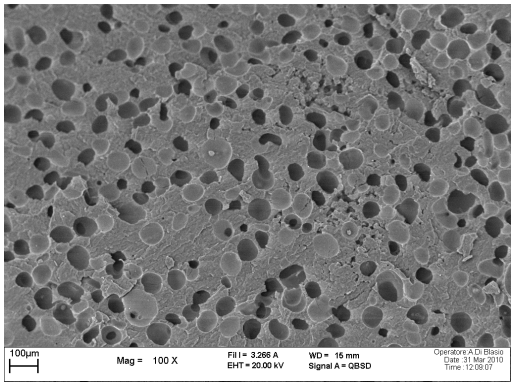

(e)

Figure 2: SEM micrographs of selectively extracted blends of PVDF/PPgMA 9/1 (a), PVDF/PPgMA 8/2 (b), PVDF/PPgMA 7/3 (c), PVDF/PPgMA 6/4 (d) and PVDF/PPgMA 5/5 (e).

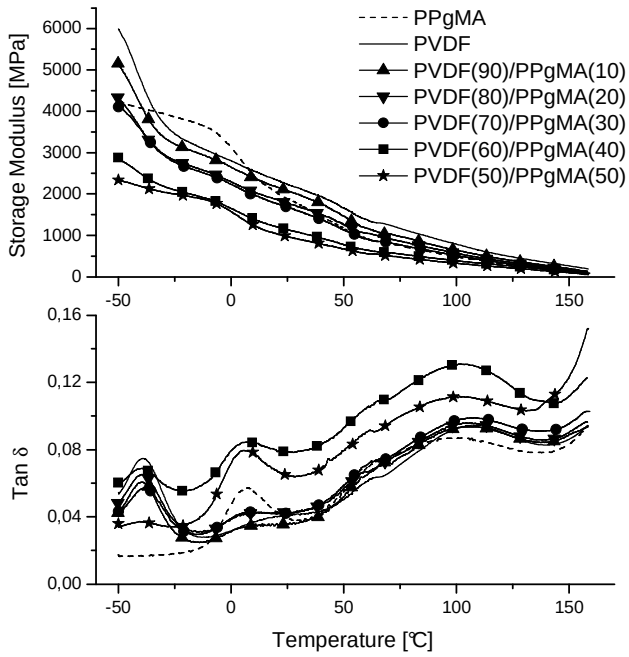

Figure 3: Temperature dependence of storage modulus and tanδ of PVDF/PPgMA blends at different compositions

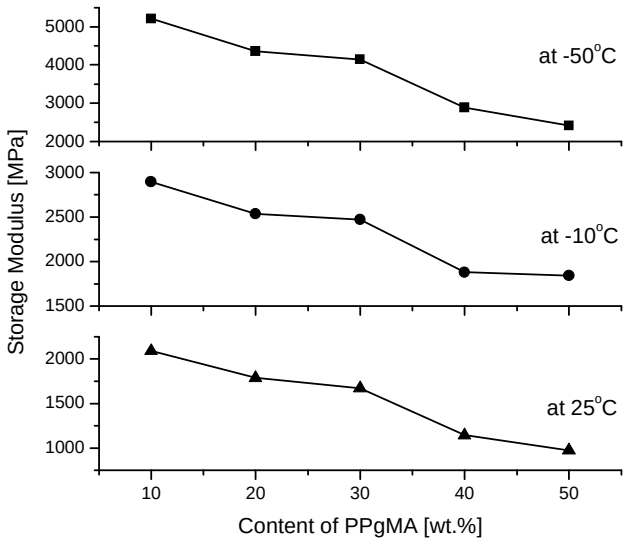

Figure 4: Storage modulus as a function of the content of PPgMA at -50, -10 and 25°C

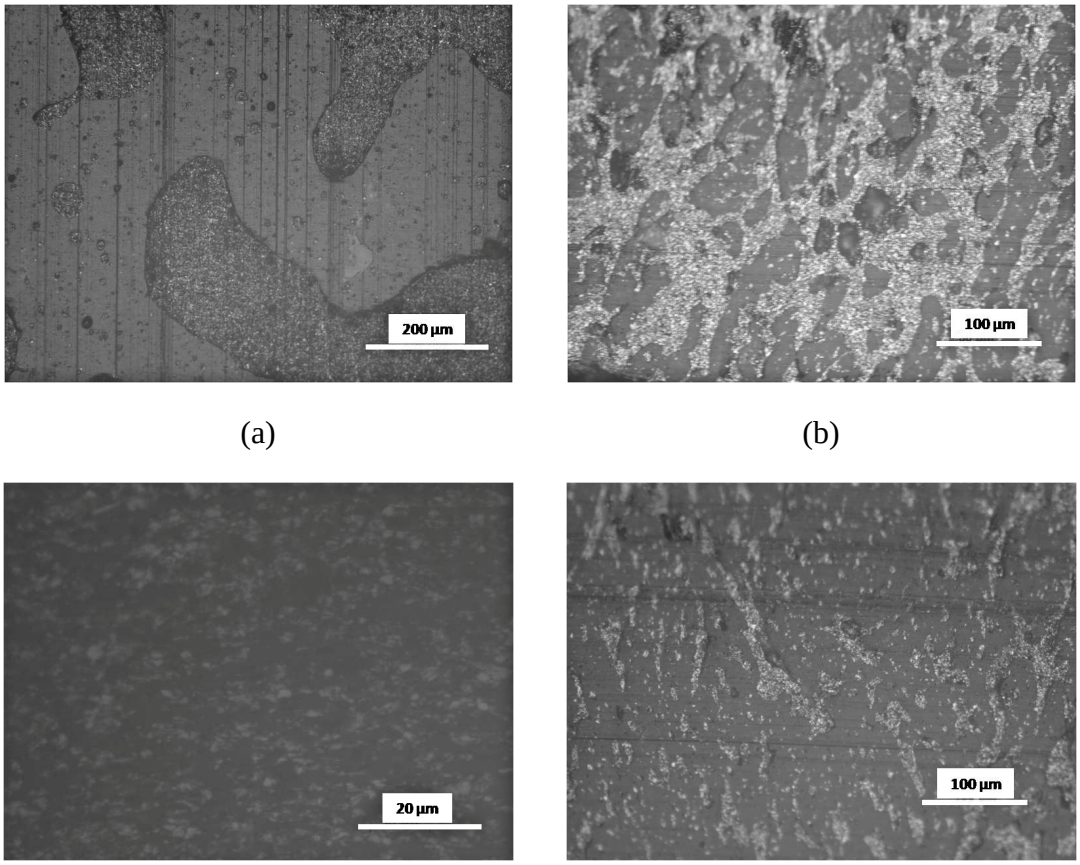

Figure 5: Optical micrographs of PVDF/PPgMA/Graphite composites: PVDF(63)/PPgMA(27)/Graph(10) (a), PVDF(56)/PPgMA(24)/Graph(20) (b), PVDF(49)/PPgMA(21)/Graph(30) (c) and PVDF(77)/PPgMA(13)/Graph(10) (d).

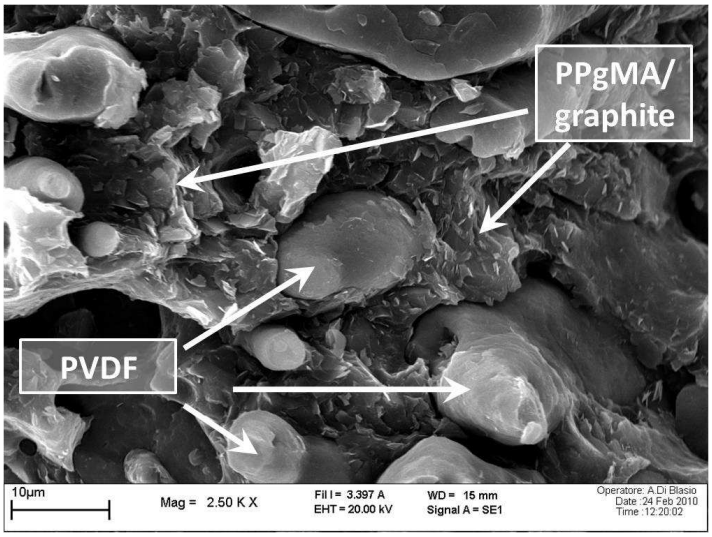

Figure 6: SEM micrograph for PVDF(56)/PPgMA(24)/Graph(20). PVDF and PPgMA/graphite domains are highlighted by the arrows in the picture.

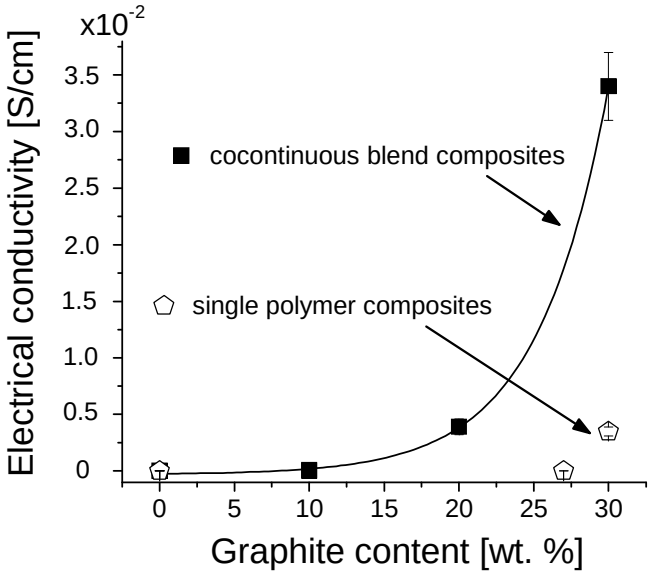

Figure 7: Electrical conductivity vs. graphite content for single polymer composites and cocontinuous blend composites. Data are reported with experimental deviations between repeated tests.

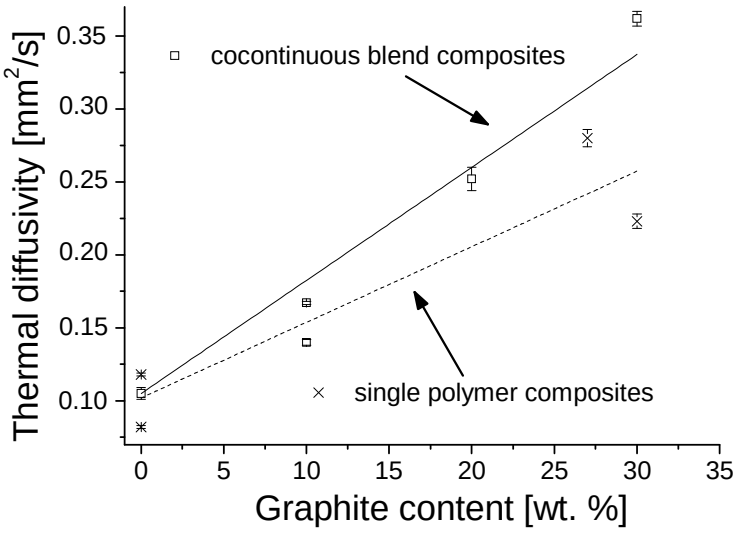

Figure 8: Thermal diffusivity vs. graphite content for single polymer composites and cocontinuous blend composites. Data are reported with experimental deviations between repeated tests and their linear fitting.